PTHR1 Loss-of-Function Mutations in Familial, Nonsyndromic Primary Failure of Tooth Eruption

Eva Decker,[1,2,6] Angelika Stellzig-Eisenhauer,[3,6] Britta S. Fiebig,[1] Christiane Rau,[3] Wolfram Kress,[4] Kathrin Saar,[5] Franz Rüschendorf,[5] Norbert Hubner,[5] Tiemo Grimm,[4] and Bernhard H.F. Weber[1,*]

Tooth eruption is a complex developmental process requiring coordinated navigation through alveolar bone and oral epithelium. Primary failure of tooth eruption (PFE) is associated with several syndromes primarily affecting skeletal development, but it is also known as a nonsyndromic autosomal-dominant condition. Teeth in the posterior quadrants of the upper and lower jaw are preferentially affected and usually result in an open bite extending from anterior to posterior. In this study, we show that familial, nonsyndromic PFE is caused by heterozygous mutations in the gene encoding the G protein-coupled receptor for parathyroid hormone and parathyroid hormone-like hormone (PTHR1). Three distinct mutations, namely c.1050-3C > G, c.543+1G > A, and c.463G > T, were identified in 15 affected individuals from four multiplex pedigrees. All mutations truncate the mature protein and therefore should lead to a functionless receptor, strongly suggesting that haplo-insufficiency of PTHR1 is the underlying cause of nonsyndromic PFE. Although complete inactivation of *PTHR1* is known to underlie the autosomal-recessive Blomstrand osteochondrodysplasia (BOCD), a lethal form of short-limbed dwarfism, our data now imply that dominantly acting PTHR1 mutations that lead to haplo-insufficiency of the receptor result in a nonsyndromic phenotype affecting tooth development with high penetrance and variable expressivity.

Nonsyndromic primary failure of tooth eruption (PFE) is a rare condition that has high penetrance and variable expressivity and in which tooth retention occurs without evidence of any obvious mechanical interference (Figure S1 in the Supplemental Data available online).[1,2] Instead, malfunction of the eruptive mechanism itself appears to cause nonankylosed permanent teeth to fail to erupt, although the eruption pathway has been cleared by bone resorption. Teeth in the posterior quadrants of the upper and lower jaw are preferentially affected, and this usually results in a progressive open bite extending from anterior to posterior (Figure 1A). Nonankylosed teeth tend to become ankylosed, i.e., the root directly fuses to the jawbone when mechanical forces are applied, rendering orthodontic treatment of affected teeth generally unsuccessful.

We have identified four families, each with at least two members affected by nonsyndromic PFE in successive generations, strongly suggesting dominant transmission of the underlying defect (Figure 1B and Table 1). The patients were referred to the Department of Orthodontics at the University of Wuerzburg Dental Clinic by local dentists, orthodontists, and oral surgeons because of eruption disturbances in permanent teeth. All subjects considered themselves to be in good health and had no history of any relevant medical condition, dental trauma, inflammation of the relevant alveolar area, or congenital anomalies such as cleft lip and palate or craniofacial malformations. In addition, index patients of family ZD1 (III:2) and ZD3 (II:1) were carefully examined in the course of a genetic-counseling session by one of the authors (B.S.F). Physical examination of both patients did not reveal any exceptional skeletal deformation or enchondromatosis. Medical history suggested neither hypo- nor hyperparathyroidism. Patient III:2 (height 1.86 m, age 27) underwent surgery of unilateral club foot at the age of one year. Patient II:1 (height 1.89 m, age 23) exhibited a leptosomic body stature and a minimal pectus carinatum. The study followed the tenets of the Declaration of Helsinki and was approved by the local ethics committee of the University of Wuerzburg (study ID 103/04). Blood samples for genetic analysis were taken only after each patient received a detailed explanation of the nature and possible consequences of the study and granted informed consent.

A standardized assessment, including clinical and radiographic examinations, of the dental condition of all patients was performed. In general, a dental panoramic tomography was available. In accordance with Proffit and Vig[1], characteristic features of primary failure of eruption included (1) posterior more than anterior tooth involvement, (2) varying degrees of abnormalities presenting distally to the first tooth involved, (3) eruption of involved teeth all the way into occlusion followed by cessation to erupt; or failure to erupt even though the overlying bone was removed by apparently normal resorption to provide an eruption pathway, and (4) no response of involved teeth to orthodontic forces. All characteristics (1) to (4) were present in 13 of the 15 patients. No patient who had undergone orthodontic treatment saw any improvement. In the remaining two patients (ZD2-I:2; ZD3-I:1, see Table 1), affected teeth had probably been removed in the past by dentists or oral surgeons.

[1]Institute of Human Genetics, University of Regensburg, Regensburg 93053, Germany; [2]Institute of Human Genetics, University of Heidelberg, Heidelberg 69120, Germany; [3]Department of Orthodontics, University of Würzburg, Würzburg 97070, Germany; [4]Institute of Human Genetics, University of Würzburg, Würzburg 97074, Germany; [5]Max Delbrück Center for Molecular Medicine, Berlin 13092, Germany
[6]These authors contributed equally to this work
*Correspondence: bweb@klinik.uni-regensburg.de
DOI 10.1016/j.ajhg.2008.11.006.

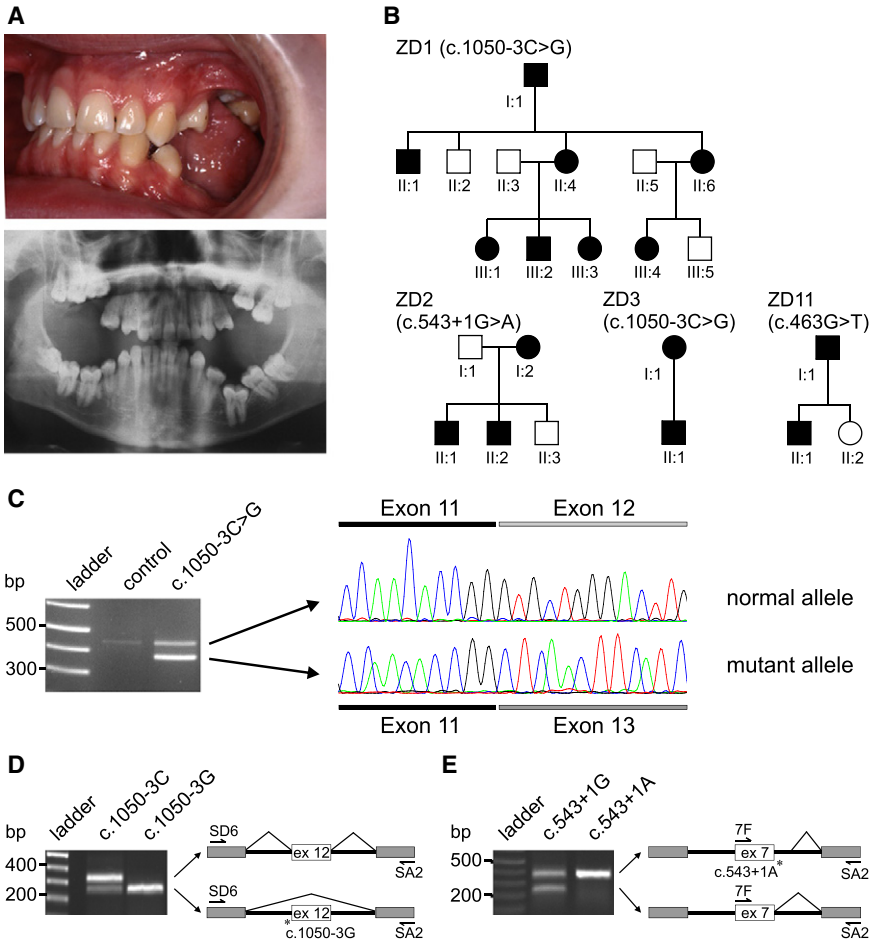

Figure 1. *PTHR1* Mutations in Individuals Affected by Nonsyndromic PFE and Their Effect on Transcript Splicing

(A) Eruption failure of posterior teeth and deficits in alveolar bone growth result in a severe bilateral open bite. Shown are an intraoral view (upper chart) and orthopantomogram (lower chart) of patient ZD1-III:2.

(B) Pedigree drawings showing individuals examined clinically and by mutation analysis. *PTHR1* mutations segregating with the clinical phenotype are presented in brackets.

(C) RT-PCR analysis of splice-site mutation c.1050-3C > G in gingival RNA of patient ZD1-III:3. Sequence traces of the normal allele and the shortened mutant allele demonstrate the excision of exon 12 in the mature transcript of the mutated allele.

(D) In vitro minigene reporter analysis of splice-acceptor sequence mutation c.1050-3C > G. Irregular transcript splicing is observed for the mutant allele such that the entire *PTHR1* exon 12 is skipped.

(E) In vitro minigene reporter analysis of splice-donor sequence mutation c.543+1G > A. Irregular transcript splicing involving a vector-specific cryptic splice is observed for the mutant allele.

In one of the multiplex families (ZD1, see Figure 1B), DNA samples of eight affected and four unaffected members were genotyped wih the Affymetrix Human Mapping 250K StyI array and were used for analysis aimed at establishing chromosomal linkage to disease. For each individual, an aliquot of 250 ng genomic DNA was digested with StyI, an adaptor was ligated, and molecules were amplified by PCR, purified, fragmented, and labeled with biotin. The cocktail was then hybridized to the StyI array, which contains roughly 238,000 SNPs. Genotype calling was performed with Affymetrix software GTYPE v4.1. The QC call rate performed with the Dynamic Model algorithm (DM) was above the 93% DM call-rate threshold for all samples, and samples were further analyzed with the Bayesian Robust Linear Model including the Mahalanobis distance classifier (BRLMM).[3] For final data analysis, only genotypes with a BRLMM confidence threshold of less than 0.3 were included.

Quality control and data conversion were managed by ALOHOMORA.[4] The correct relationship of individuals within the families was checked with the software Graphical Representation of Relationships (GRR).[5] For GRR, we selected 14,339 SNPs, distributed on the autosomes, with a minimal distance of 200 kbp between markers and a minimal minor allele frequency of 0.1 in Europeans. For each pair of individuals, GRR calculates over the 14,339 markers the Identical-by-State (IBS) mean and standard deviation. The graphical plot of IBS mean versus IBS standard deviation facilitates distinguishing between parents and offspring, siblings, half siblings, and cousins, as well as identical or unrelated individuals. SNPs with Mendelian errors were detected by PedCheck[6], and genotypes were deleted in all individuals; unlikely genotypes (double recombinants), identified with Merlin,[7] were deleted in the individuals where they appeared. For parametric multipoint LOD score analysis and haplotyping, Merlin was used with complete penetrance and a trait locus allele frequency of 0.001. Marker allele frequencies for a European population as well as genetic positions were extracted from the Affymetrix SNP annotation file (version na21). From 238,304 SNPs on the array, 238,230 had a physical and genetic position. To reduce the impact of Linkage Disequilibrium (LD) between closely linked markers on the LOD score analysis, we recalculated the pedigree with smaller sets of markers (136,390 and 82,918 SNPs, respectively) such that there was a minimal distance of 1,000 and 10,000 bp between neighboring markers.

Parametric linkage analysis with a dominant model revealed two regions with a maximal LOD score of 2.41, a 31.8 Mbp interval between flanking markers rs1402366 and rs13074914on chromosome 3p14.3-p24.3, and an 8.0 Mbp interval flanked by markers rs1328369 and

Table 1. Characterization of Family Members with *PTHR1* Mutations

Family ID	Pedigree Position[c]	Height (m)[d]	Nucleotide Change	Amino Acid Change	Affected Teeth[a]																				
					Upper Right[b]					Upper Left[b]					Lower Left[b]					Lower Right[b]				
					8	7	6	5	4	8	7	6	5	4	8	7	6	5	4	8	7	6	5	4
ZD1	I:1	1.70	c.1050-3C > G	p.Cys351SerfsX133	·	·	·	·	·	■	■	·	·	·	·	·	·	·	·	×	■	■	·	·
	II:1	1.82	c.1050-3C > G	p.Cys351SerfsX133	■	■	■	■	■	■	■	■	■	·	■	■	■	·	■	■	■	■	■	■
	II:2	n.a.	no	no																				
	II:3	n.a.	no	no																				
	II:4	1.65	c.1050-3C > G	p.Cys351SerfsX133	■	■	×	·	·	■	■	×	■	■	■	■	×	×	■	■	×	■	·	·
	II:5	n.a.	no	no																				
	II:6	1.62	c.1050-3C > G	p.Cys351SerfsX133	×	■	■	·	·	·	·	·	·	·	·	·	·	·	·	×	■	×	·	·
	III:1	1.70	c.1050-3C > G	p.Cys351SerfsX133	■	■	■	■	■	■	■	■	■	·	■	■	■	■	·	■	■	■	■	·
	III:2	1.88	c.1050-3C > G	p.Cys351SerfsX133	■	■	■	■	■	■	■	■	■	■	■	■	■	■	■	■	■	■	■	■
	III:3	1.72	c.1050-3C > G	p.Cys351SerfsX133	·	·	·	·	·	·	·	·	·	·	■	■	■	■	·	·	·	·	·	·
	III:4	1.70	c.1050-3C > G	p.Cys351SerfsX133	■	■	■	■	■	■	■	■	■	■	■	■	■	■	■	·	·	·	·	·
	III:5	n.a.	no	no																				
ZD2	I:1	1.82	no	no																				
	I:2	1.78	c.543+1G > A	p.Glu182ValfsX20	×	×	·	·	·	×	×	·	·	·	×	×	×	·	·	·	·	·	·	×
	II:1	1.96	c.543+1G > A	p.Glu182ValfsX20	■	■	■	■	·	■	■	■	■	■	·	·	·	·	·	·	·	·	·	·
	II:2	1.93	c.543+1G > A	p.Glu182ValfsX20	·	·	·	·	·	·	·	·	·	·	·	·	·	·	·	■	■	■	■	·
	II:3	1.75	no	no																				
ZD3	I:1	1.70	c.1050-3C > G	p.Cys351SerfsX133	×	×	·	·	·	·	·	·	×	·	×	×	×	·	·	·	·	×	·	×
	II:1	1.89	c.1050-3C > G	p.Cys351SerfsX133	■	■	■	■	■	■	■	■	■	■	■	■	■	·	·	■	■	■	·	·
ZD11	I:1	1.86	c.463G > T	p.Glu155Ter	·	·	×	·	·	■	■	■	■	·	·	·	×	×	·	■	■	■	·	·
	II:1	1.80	c.463G > T	p.Glu155Ter	■	■	■	■	■	■	■	■	■	■	■	■	■	■	·	■	■	■	■	·
	II:2	n.a.	no	no																				

[a] Tooth present (·), not present (×), or affected (■). No entry means there was no information.
[b] 4 = first premolar; 5 = second premolar; 6 = first molar; 7 = second molar; and 8 = third molar.
[c] See Figure 1.
[d] n.a. = not available.

rs7988100 on chromosome 13q31.3-q33.1 (Figures S2–S4). The latter region includes 31 known protein-coding genes as defined by the NCBI mRNA reference sequences collection (RefSeq) presently totaling 445 exons (Table S1). Of these, 423 coding exons and their respective adjacent splice acceptor and donor sites were analyzed by direct sequencing of patients ZD1-II:4 and ZD1-III:3, as well as individual ZD1-II:3 as an unaffected control. No disease-associated mutation could be detected, thus effectively excluding 13q31.3-q33.1 as a PFE candidate region.

The second interval of interest on 3p harbors 301 RefSeq genes (Table S2), making a systematic exon-sequencing strategy unfeasible. We therefore selected candidates from the chromosomal region on the basis of a number of criteria, such as expression in bone or bone-associated tissue, functional considerations of the encoded protein, and a known role in disease processes or animal models of disease. Under this approach, one of the candidates encoding the parathyroid hormone receptor 1 (PTHR1 [MIM 168468]) appeared to be a good positional candidate for PFE for several reasons. PTHR1 is a member of the G protein-coupled receptor family class B (secretin-like) and binds parathyroid hormone (PTH [MIM 168450]) and parathyroid hormone-like hormone (PTHLH [MIM 168470]) with equal affinity.[8] In tooth development, *PTHLH* expression is restricted to the epithelial layer, whereas *PTHR1* expression is found in both the adjacent dental mesenchyme and in the alveolar bone.[9,10] In addition, gene-manipulated mice deficient for either PTHR1 or PTHLH die perinatally,[11,12] but transgenic rescue of the *PTHLH* knockout mice by either chondrocyte-targeted expression of *PTHLH*[9] or constitutive expression of *PTHR1*[13] results in viable animals with dysmorphic features, including failure of tooth eruption. This strongly points to a role of PTHLH and/or PTHR1 signaling in the regulation of epithelial-mesenchymal interactions during the development of epithelial organs such as teeth. Finally, Blomstrand osteochondrodysplasia (BOCD), a lethal form of short-limbed dwarfism, has long been known to be associated with recessive, loss-of-function mutations in the *PTHR1* gene.[14–19] In addition to skeletal anomalies, the clinical features of BOCD were recently reevaluated and shown to include severe abnormalities in tooth morphogenesis.[20] In two affected fetuses, deciduous teeth were present but severely impacted within the surrounding alveolar bone, leading to distortions in their architecture and orientation.

Consequently, we analyzed all 14 *PTHR1* coding exons and the respective intron-exon boundaries by direct sequencing (Table S3) and identified three novel heterozygous mutations in each of the four multiplex pedigrees (Figure 1B and Table 1). Affected individuals, but not those without pathological findings, harbored the splice junction mutation c.1050-3C > G (families ZD1 and ZD3) or c.543+1G > A (family ZD2) or the nonsense mutation

c.463G > T (family ZD11) (Figure 1B). The latter change directly results in a termination codon and truncates the PTHR1 protein at amino acid position 155 (p.Glu155Ter). Haplotyping at the *PTHR1* locus revealed that mutation c.1050-3C > G originates from a common founder in families ZD1 and ZD3, and all affected individuals share an extended haplotype (Figure S5). Mutations c.543+1G > A and c.463G > T were analyzed in 178 control individuals of German descent[21] by PCR amplification with primer pair PTHR1-RNA-ex6F (5′-GGA ATG GGA CCA CAT CCT GT-3′) and BamHI-PTHR1-ex7R (5′-CGC GGA TCC TGG GGT GGG AGT GAA TTT AT-3′) and subsequent direct sequencing with primer PTHR1-RNA-ex6F. The c.1050-3C > G mutation in *PTHR1* exon 12 was amplified by PCR in the same 178 controls with primer pair PTHR1-ex12F (Table S3) and PTHR1-ex12R2 (5′-CAG AGA TGC AGT GAC AGA GC-3′) and tested for the presence of the nucleotide change by restriction enzyme digestion with BstNI. None of the three mutations identified in our PFE patients was found in the 178 controls (356 alleles), formally excluding the possibility that one of these changes represents a rare polymorphic variant in the general population.

The functional effect of splice junction mutation c.1050-3C > G on transcript splicing was further analyzed in gingival RNA from patient ZD1-III:3 (Figures 1B and 1C). Total RNA was isolated, and first-strand complementary DNA was generated from total RNA by reverse transcription (RT). This DNA served as a template in subsequent RT-PCR reactions. PCR products were generated with exonic primers PTHR1-RNA-ex10F (5′-GAA GTA CCT GTG GGG CTT CA-3′) and PTHR1-RNA-ex15R (5′-TCG CCA TTG CAG AAA CAG TA-3′). After agarose gel excision and purification, PCR products were cycle sequenced. Compared to a control transcript, the mutant allele results in a complete exclusion of exon 12, thus fusing *PTHR1* exon 11 to exon 13 (Figure 1C). This should cause a frame shift at codon 351 and thus create a new reading frame that encodes an additional, PTHR1-unrelated 133 C-terminal amino acid (p.Cys351SerfsX133). The skipping of the entire exon 12 as a result of the c.1050-3C > G mutation was further confirmed in an in vitro minigene reporter assay that is based on COS7 cell expression of normal and mutant alleles in the context of flanking reporter exons (Figure 1D).

Because gingival tissue was unavailable from affected members of family ZD2, *PTHR1* mutation c.543+1G > A was analyzed via the minigene reporter assay. The region encompassing the affected splice site and the adjacent exon(s) was amplified from the patient's genomic DNA by PCR with oligonucleotide primer pairs EcoRI-PTHR1-ex7F (5′-CCG GAA TTC TTG GAG CTA GGG GTT CAG TG-3′) and BamHI-PTHR1-ex7R. Coupling EcoRI and BamHI recognition sequences to the forward and reverse primers, respectively, ensured directional insertion into the pSPL3b vector (GIBCO, Life Technology, Eggenstein, Germany). Wild-type and mutant clones were selected for transformation into COS7 cells. After 24 hr, mRNA was isolated from the COS7 cells and analyzed by RT-PCR with exonic primer PTHR1-RNA-ex7F (5′-GCC TGG GCA CAA CAG GAC-3′) and vector primer SA2 (5′-ATC TCA GTG GTA TTT GTG AGC-3′). The RT-PCR products were sequenced and demonstrated the loss of the donor splice site of entire exon 7 (Figure 1E), thus predicting a frame shift and a premature termination of the protein (p.Glu182ValfsX20).

Mutations in the *PTHR1* gene have been associated with a number of clinically distinct skeletal disorders. Complete or almost complete inactivation of both *PTHR1* alleles is associated with autosomal-recessive BOCD, a skeletal dysplasia with advancement of bone maturation.[14–20] In contrast, autosomal-dominant gain-of-function mutations in *PTHR1* lead to short-limb dwarfism, known as Jansen metaphyseal chondrodysplasia, and characterized by a retarded differentiation of chondrocytes.[22] Clinically, this phenotype can be confused with hyperparathyroidism. Another condition called enchondromatosis, or Ollier disease, which can manifest as multiple cartilage tumors and is frequently associated with skeletal deformity, can be caused by autosomal-dominant missense mutations in the *PTHR1* gene.[23] Finally, Eiken syndrome, a rare autosomal-recessive skeletal dysplasia, is characterized by multiple epiphyseal dysplasia and extremely retarded ossification and differs from Jansen and Blomstrand chondrodysplasia and from enchondromatosis.[18] The autosomal-dominant *PTHR1* mutations identified in our families with nonsyndromic PFE truncate the mature receptor protein before the first transmembrane domain (TM) (p.Glu182ValfsX20; p.Glu155Ter) or eliminate the fifth, sixth, and seventh TM, the connecting intracellular and extracellular loops, and the cytoplasmic tail (p.Cys351SerfsX133). In all cases, the mutations should lead to premature proteolytic degradation of the precursor protein or to a functionless receptor, thus suggesting that haploinsufficiency of PTHR1 is likely to be the underlying principle of nonsyndromic PFE. Interestingly, PFE has not been reported as a symptom in heterozygous carriers of autosomal-recessive BOCD.[14–20] This may, however, be explained by an incomplete medical history of the carrier parents of BOCD fetuses. PFE is now the fifth disease associated with mutations in the *PTHR1* gene further highlighting the fact that this receptor has multiple functional aspects that can be disrupted by mutations acting in defined and specific modes leading to the various associated diseases. A similarly complex pattern of genotype-phenotype correlation was shown in other skeletal disorders, such as the *FGFR*-associated craniosynostosis.[24]

In both BOCD patients[20] and rescued *PTHLH*-transgenic *PTHLH* knockout mice[9], tooth buds appear to develop normally, and it appears that there is regular secretion and maturation of dentine and enamel during the crown stage of tooth development. It is only later that progressive distortion of teeth and failure to erupt become evident, indicating that subtle disturbances in alveolar bone resorption may prevent the formation of an eruption pathway. By the time an eruption pathway forms, the alveolar bone surface

is mainly covered by osteoclasts (bone resorption), whereas osteoblasts (bone formation) are virtually absent.[25] Because nonsyndromic PFE patients do not show any signs of peripheral skeleton abnormalities, a systemic impairment of osteoclast formation or function as a result of PTHR1 haploinsufficiency appears unlikely. Rather, nonsyndromic PFE might be attributable to a threshold-dependent disturbance in crosstalk between mesenchymal and epithelial cells in the immediate vicinity of the eruption pathway, and this disturbance might impair the delicate balance of bone resorption and formation. Because osteoclasts do not appear to express functional PTHR1 receptors at their cell surfaces,[26,27] paracrine or juxtacrine signaling mediated by PTHR1 receptor-positive cells, e.g., in the dental follicular mesenchyme, needs to be considered.

Supplemental Data

Five figures and three tables are available with this article online at http://www.ajhg.org/.

Acknowledgments

We are grateful to the patients and their families for their participation in this study and to Yana Walczak (Institute of Human Genetics, University of Regensburg, Germany) for helping with RNA extraction. This work was supported in part by a grant from the German Orthodontic Society (DGKFO) and the German Ministry of Science and Education (NGFN2).

Received: September 21, 2008
Revised: November 8, 2008
Accepted: November 11, 2008
Published online: December 4, 2008

Web Resources

The URLs for data presented herein are as follows:

Affymetrix SNPannotation file, Mapping250K_Sty.na21.annot.csv http://www.affymetrix.com/support/technical/byproduct.affx?product=500k
ALOHOMORA, http://gmc.mdc-berlin.de/alohomora/
GRR, http://www.sph.umich.edu/csg/abecasis/GRR/index.html
Merlin, http://www.sph.umich.edu/csg/abecasis/Merlin/
Online Mendelian Inheritance in Man (OMIM), http://www.ncbi.nlm.nih.gov/Omim/
PedCheck, http://watson.hgen.pitt.edu/register/soft_doc.html

References

1. Proffit, W.R., and Vig, K.W. (1981). Primary failure of eruption: A possible cause of posterior open-bite. Am. J. Orthod. *80*, 173–190.
2. Raghoebar, G.M., Boering, G., Vissink, A., and Stegenga, B. (1991). Eruption disturbances of permanent molars: A review. J. Oral Pathol. Med. *20*, 159–166.
3. Rabbee, N., and Speed, T.P. (2006). A genotype calling algorithm for affymetrix SNP arrays. Bioinformatics *22*, 7–12.
4. Rüschendorf, F., and Nürnberg, P. (2005). ALOHOMORA: A tool for linkage analysis using 10K SNP array data. Bioinformatics *21*, 2123–2125.
5. Abecasis, G.R., Cherny, S.S., Cookson, W.O.C., and Cardon, L.R. (2001). GRR: Graphical representation of relationship errors. Bioinformatics *17*, 742–743.
6. O'Connell, J.R., and Weeks, D.E. (1998). PedCheck: A Program for identification of genotype incompatibilities in linkage analysis. Am. J. Hum. Genet. *63*, 259–266.
7. Abecasis, G.R., Cherny, S.S., Cookson, W.O.C., and Cardon, L.R. (2002). MERLIN—Rapid analysis of dense genetic maps using sparse gene flow trees. Nat. Genet. *30*, 97–101.
8. Jüppner, H., Abou-Samra, A.B., Freeman, M., Kong, X.F., Schipani, E., Richards, J., Kolakowski, L.F., Hock, J., Potts, J.T., Kronenberg, H.M., et al. (1991). A G protein-linked receptor for parathyroid hormone and parathyroid hormone-related peptide. Science *254*, 1024–1026.
9. Philbrick, W.M., Dreyer, B.E., Nakchbandi, I.A., and Karaplis, A.C. (1998). Parathyroid hormone-related protein is required for tooth eruption. Proc. Natl. Acad. Sci. USA *95*, 11846–11851.
10. Calvi, L.M., Shin, H.I., Knight, M.C., Weber, J.M., Young, M.F., Giovannetti, A., and Schipani, E. (2004). Constitutively active PTH/PTHrP receptor in odontoblasts alters odontoblast and ameloblast function and maturation. Mech. Dev. *121*, 397–408.
11. Karaplis, A.C., Luz, A., Glowacki, J., Bronson, R.T., Tybulewicz, V.L., Kronenberg, H.M., and Mulligan, R.C. (1994). Lethal skeletal dysplasia from targeted disruption of the parathyroid hormone-related peptide gene. Genes Dev. *8*, 277–289.
12. Lanske, B., Karaplis, A.C., Lee, K., Luz, A., Vortkamp, A., Pirro, A., Karperien, M., Defize, L.H., Ho, C., Mulligan, R.C., et al. (1996). PTH/PTHrP receptor in early development and Indian hedgehog-regulated bone growth. Science *273*, 663–666.
13. Schipani, E., Lanske, B., Hunzelman, J., Luz, A., Kovacs, C.S., Lee, K., Pirro, A., Kronenberg, H.M., and Jüppner, H. (1997). Targeted expression of constitutively active receptors for parathyroid hormone and parathyroid hormone-related peptide delays endochondral bone formation and rescues mice that lack parathyroid hormone-related peptide. Proc. Natl. Acad. Sci. USA *94*, 13689–13694.
14. Jobert, A.S., Zhang, P., Couvineau, A., Bonaventure, J., Roume, J., Le Merrer, M., and Silve, C. (1998). Absence of functional receptors for parathyroid hormone and parathyroid hormone-related peptide in Blomstrand chondrodysplasia. J. Clin. Invest. *102*, 34–40.
15. Zhang, P., Jobert, A.S., Couvineau, A., and Silve, C. (1998). A homozygous inactivating mutation in the parathyroid hormone/parathyroid hormone-related peptide receptor causing Blomstrand chondrodysplasia. J. Clin. Endocrinol. Metab. *83*, 3365–3368.
16. Karaplis, A.C., He, B., Nguyen, M.T., Young, I.D., Semeraro, D., Ozawa, H., and Amizuka, N. (1998). Inactivating mutation in the human parathyroid hormone receptor type 1 gene in Blomstrand chondrodysplasia. Endocrinology *139*, 5255–5258.
17. Karperien, M., van der Harten, H.J., van Schooten, R., Farih-Sips, H., den Hollander, N.S., Kneppers, S.L., Nijweide, P., Papapoulos, S.E., and Löwik, C.W. (1999). A frame-shift mutation in the type I parathyroid hormone (PTH)/PTH-related peptide receptor causing Blomstrand lethal osteochondrodysplasia. J. Clin. Endocrinol. Metab. *84*, 3713–3720.
18. Duchatelet, S., Ostergaard, E., Cortes, D., Lemainque, A., and Julier, C. (2005). Recessive mutations in PTHR1 cause contrasting skeletal dysplasias in Eiken and Blomstrand syndromes. Hum. Mol. Genet. *14*, 1–5.
19. Hoogendam, J., Farih-Sips, H., Wÿnaendts, L.C., Löwik, C.W., Wit, J.M., and Karperien, M. (2007). Novel mutations in the

parathyroid hormone (PTH)/PTH-related peptide receptor type 1 causing Blomstrand osteochondrodysplasia types I and II. J. Clin. Endocrinol. Metab. *92*, 1088–1095.

20. Wysolmerski, J.J., Cormier, S., Philbrick, W.M., Dann, P., Zhang, J.P., Roume, J., Delezoide, A.L., and Silve, C. (2001). Absence of functional type 1 parathyroid hormone (PTH)/PTH-related protein receptors in humans is associated with abnormal breast development and tooth impaction. J. Clin. Endocrinol. Metab. *86*, 1788–1794.
21. Rivera, A., Fisher, S.A., Fritsche, L.G., Keilhauer, C.N., Lichtner, P., Meitinger, T., and Weber, B.H. (2005). Hypothetical LOC387715 is a second major susceptibility gene for age-related macular degeneration, contributing independently of complement factor H to disease risk. Hum. Mol. Genet. *14*, 3227–3236.
22. Schipani, E., and Provot, S. (2003). PTHrP, PTH, and the PTH/PTHrP receptor in endochondral bone development. Birth Defects Res. C. Embryo Today. *69*, 352–362.
23. Couvineau, A., Wouters, V., Bertrand, G., Rouyer, C., Gérard, B., Boon, L.M., Grandchamp, B., Vikkula, M., and Silve, C. (2008). PTHR1 mutations associated with Ollier disease result in receptor loss of function. Hum. Mol. Genet. *17*, 2766–2775.
24. Wilkie, A.O., Patey, S.J., Kan, S.H., van den Ouweland, A.M., and Hamel, B.C. (2002). FGFs, their receptors, and human limb malformations: clinical and molecular correlations. Am. J. Med. Genet. *112*, 266–278.
25. Marks, S.C., Cahill, D.R., and Wise, G.E. (1983). The cytology of the dental follicle and adjacent alveolar bone during tooth eruption in the dog. Am. J. Anat. *168*, 277–289.
26. Mundy, G.R., and Roodman, G.D. (1987). In Bone and Mineral Research, Volume *5*, W.A. Peck, ed. (Amsterdam: Elsevier), pp. 209–280.
27. Martin, T.J., Ng, K.W., and Suda, T. (1989). In Metabolic Bone Disease, I. Part and R.D. Tiegs, eds. (Philadelphia: Saunders), pp. 833–858.